Ultrasonics Sonochemistry 102 (2024) 106736

Contents lists available at ScienceDirect

Ultrasonics Sonochemistry

journal homepage: www.elsevier.com/locate/ultson

Optimizing sludge dewatering efficiency with ultrasonic Treatment: Insights into Parameters, Effects, and microstructural changes

Yongzheng Qi [a,b,c,*], Jianhao Chen [a], Haoqing Xu [a,c], Silin Wu [a,c], Ziming Yang [a], Aizhao Zhou [a,c], Yunjie Hao [a]

[a] *Jiangsu University of Science and Technology, School of Civil Engineering and Architecture, Zhenjiang 212003, PR China*
[b] *The National Key Laboratory of Water Disaster Prevention, Nanjing 210029, PR China*
[c] *Jiangsu Province Engineering Research Center of Geoenvironmental Disaster Prevention and Remediation, Jiangsu, Zhenjiang 212100, PR China*

ARTICLE INFO

Keywords:
Ultrasonic effect
Ultrasonic energy density
Ultrasonic duration
Sludge dewatering characteristics
Sludge microstructure

ABSTRACT

Sludge dewatering plays a critical role in the efficient and cost-effective management of wastewater treatment plants. Ultrasonic treatment has emerged as a promising technique for improving dewatering processes. This study aims to evaluate the impact of ultrasonic treatment on sludge dewatering characteristics. A series of experiments were conducted to evaluate the dewatering characteristics of sludge under ultrasonic treatment. Experimental data was collected, and the effects of ultrasonic parameters on dewatering efficiency were analyzed. Ultrasound has the capacity to disintegrate sludge flocs, liberate tightly bound water, and enhance sludge dewatering capabilities. The application of ultrasound leads to the breakdown of sludge flocs, which facilitates a substantial amount of organic acids or carbonates. This, in turn, modifies the pH value of the sludge. Additionally, ultrasound induces instantaneous high temperature and pressure within the liquid phase, consequently elevating the temperature of the sludge slurry. Optimum ultrasound energy density and duration of ultrasound treatment exist. For the sludge samples analyzed in this investigation, it was determined that the optimal ultrasonic energy density is 9.8 W, while the optimal duration of ultrasound treatment is 30 s. Excessively escalating the sound energy density or prolonging the duration of ultrasound may yield unfavorable outcomes in terms of sludge dewatering effectiveness. To enhance sludge dewatering, it is crucial to select appropriate ultrasonic energy density and duration of ultrasonic treatment. This study demonstrates the positive impact of ultrasonic treatment on the dewatering characteristics of sludge. The findings provide valuable insights into the potential of ultrasonic technology for enhancing sludge dewatering.

1. Introduction

The sludge has a water content greater than or equal to 97 %, posing challenges for transportation and treatment. Therefore, sludge dewatering is necessary. However, the complex composition of sludge extracellular polymeric substances (EPS) hinders water removal from the sludge [1,2]. Enhancing dewatering performance is crucial for sludge dewatering. Efficient sludge hydrolysis involves disrupting the cell walls of decomposing sludge bacterial micelles, facilitating rapid cell fluid outflow, destabilizing the binding state of the bacterial micelles, releasing bound water, and achieving extensive sludge dewatering [3–5].

Numerous technologies, such as microwave radiation, thermal hydrolysis, ultrasound, and the development of new flocculants [6–8], have been investigated to decrease the water content of sludge. Ultrasonic treatment technology is recognized as an effective approach for enhancing sludge dewatering performance and degradability during treatment. It offers benefits such as high efficiency, stability, cleanliness, and rapid cell breakage [9,10]. A significant amount of water present in sludge can generate numerous cavitation bubbles when subjected to ultrasound. These bubbles quickly collapse, creating intense shear forces and high temperatures, effectively breaking down EPS and releasing bound water [11–13]. Ultrasound can also disrupt the floc structure and cell walls of sludge, releasing organic matter and accelerating the hydrolysis process. Additionally, ultrasound improves the sedimentation and dewatering performance of sludge. By creating a sponge-like effect on the sludge, ultrasound facilitates the flow of water through channels on the wave surface, promoting sludge particle agglomeration and

* Corresponding author.
E-mail address: zmxtree@just.edu.cn (Y. Qi).

https://doi.org/10.1016/j.ultsonch.2023.106736
Received 4 November 2023; Received in revised form 8 December 2023; Accepted 15 December 2023
Available online 16 December 2023
1350-4177/

increased particle size [14,15]. The application of ultrasound reduces the size of floc particles and disrupts the structure of bacterial micelles, converting combined water into free water [16]. The cracking of sludge by ultrasound releases free water, thereby enhancing sludge dewatering performance and stability. Moreover, ultrasound eliminates viruses, bacteria, and other harmful substances in the sludge, thus improving the leaching and recovery rates of heavy metals. Due to its unique acoustic energy characteristics, applicability, and treatment effectiveness, ultrasound technology holds great potential for sludge dewatering treatment [17,18].

The efficacy of ultrasound treatment for improving dewatering performance in sludge is influenced by factors such as ultrasound frequency, duration, acoustic energy density, pH value, mode of action, and coupling method [19,20]. Medium and low-frequency ultrasound, along with shorter treatment times, prove beneficial for sludge dewatering [21]. Ultrasound treatment enhances the solubilization of organic matter, reduces sludge viscosity, and promotes sludge uniformity [22,23].

However, certain limitations persist with current ultrasound technology, and some mechanisms regarding ultrasound sludge dewatering remain incompletely understood [24–27]. This study aims to investigate the impact of ultrasound treatment duration on sludge dewatering performance with the goal of achieving optimal treatment efficacy.

2. Material and method

2.1. Characteristics of sludge samples

The activated sludge taken from the secondary sedimentation tank of Zhenjiang's local urban sewage treatment plant was chosen for this experiment. To maintain consistent initial conditions across all test groups, the same batch of sludge was utilized. The initial water content was measured at 97.13 %, with a unit weight of 1.026 g/cm^3. Any unused sludge samples were stored in a constant temperature refrigerator set at 4 ℃ to prevent spoilage. Table 1 and Fig. 1 present the fundamental characteristics of the raw sludge. In Table 1, SV30 stands for sludge settlement ratio, which refers to the ratio of settled sludge after 30 min compared to the total volume. To determine this, 100 mL of conditioned sludge is poured into a 100 mL graduated cylinder and left to naturally settle. The volume of settled sludge is then recorded at 0, 1, 2, 3, 4, 5, 10, 15, 20, and 30 min. By observing the volume of sludge settlement, the sludge settlement ratio can be calculated as the ratio of the settled sludge volume at 30 min to the total volume. SRF stands for Specific Resistance to Filtration, which refers to the resistance per unit area when a unit mass of sludge is filtered at a certain pressure through a unit filtration area. SRF was measured according to the method described in [28].

Table 1 provides definitions of key terms used in this study. The term "d_{10}" refers to the particle size at which the cumulative distribution reaches 10 %, indicating that 10 % of all particles are smaller than this size. "d_{50}" represents the median particle size, meaning that 50 % of particles are smaller than this size. Similarly, "d_{90}" indicates the particle size at which the cumulative distribution reaches 90 %, with 90 % of particles being smaller than this size. "Mean" refers to the weighted average particle size.

2.2. Experimental apparatus

The experimental setup utilized the SM-900A ultrasonic cell crusher, manufactured by Nanjing Shunma Instrument Equipment Co., Ltd., as illustrated in Fig. 2a. The apparatus consists of the sample processing chamber located on the right-hand side and the controller positioned on the left-hand side. With the aid of the controller, one can regulate the duration and power ratio of the ultrasound. The ultrasonic power and frequency are determined by the amplitude lever, which has a diameter of 6 cm and an end diameter of 0.25 cm in this experiment, as shown in Fig. 2b. Interestingly, this particular instrument operates at a frequency of 20 kHz and boasts a rated power of 900 w.

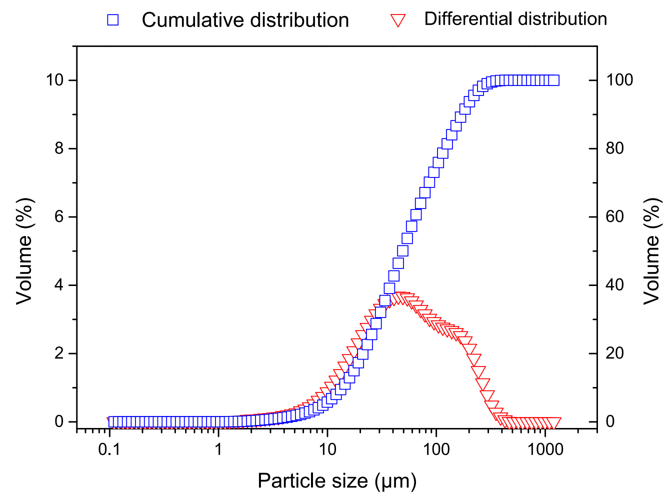

Fig. 1. Raw sludge particle size distribution.

During ultrasonic processing, the phenomenon of cavitations occurs, causing a rapid increase in liquid temperature. The temperature rise is more pronounced with higher power, smaller sample volumes. Hence, users should pay close attention to the sample temperature. It is recommended to perform short bursts of dispersing and fragmentation, with each cycle not exceeding 5 s. As a general guideline, it is suggested to operate with ultrasound on for 1–4 s and off for 2–8 s.

In addition to the aforementioned ultrasonic cell crusher, other essential instruments employed for the experiment include the LT2200E laser particle size analyzer (Zhuhai Zhenli Optical Instrument Co., Ltd., China), PXBJ-287L portable ion meter (Shanghai Leici Technology Instrument Co., Ltd., China), sludge specific resistance meter (Zhengzhou Qihua Teaching Instrument and Equipment Co., Ltd., China), JJ-4B asynchronous electric stirrer (Changzhou Weijia Instrument Manufacturing Co., Ltd., China), CS-101–2 electric drying oven (Jiulian Technology Co., Ltd., China), Coxem EM-30 PLUS desktop scanning electron microscope (Kussem, South Korea), and CR21N high-speed freezing centrifuge (Hitachi, Japan), among others.

2.3. Ultrasonic treatment experiment

Prior to conducting the experiment, 100 mL of uniform original sludge was added to a plastic bowl, which was then placed in the ultrasonic cell crusher. The amplitude lever is inserted into the sample processing chamber through the hole at the top of the chamber. Then, the end of the amplitude lever is submerged about 5 cm deep into the sludge sample. Subsequently, the controller is turned on, and the end of the amplitude lever vibrates to release ultrasonic waves, which are used for ultrasonic treatment of the sludge. Ultrasound with a frequency of 20 kHz was utilized, and the ultrasonic processing time was set to 15 s and 30 s, respectively. The ultrasonic energy density (=rated power ×

Table 1
Raw sewage sludge characteristics.

Moisture content (%)	pH	SV30 %	Density g/cm^3	Temperature (°C)	SRF, ×10^{13} m/kg	d_{10} μm	d_{50} μm	d_{90} μm	Mean μm
97.13	8.87	54	1.026	24.1 ± 2	4.76	13.680	49.129	172.116	73.109

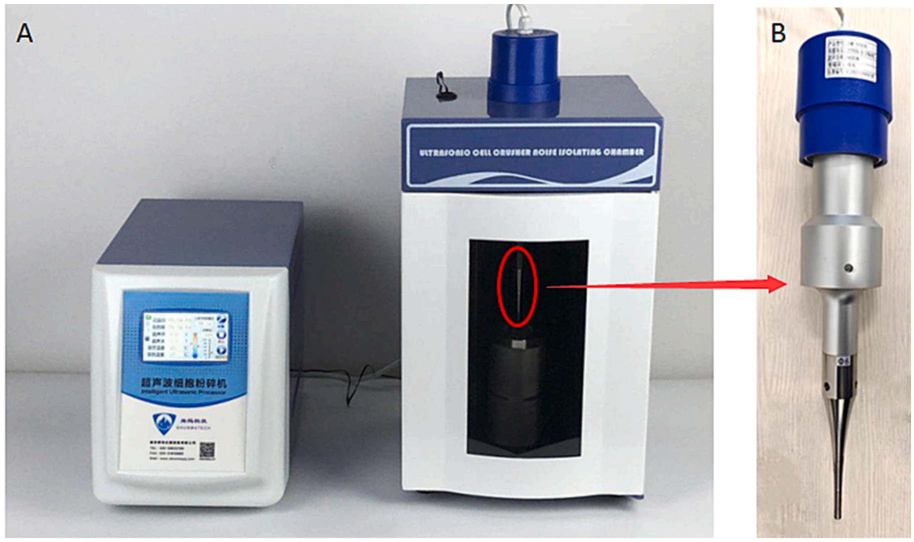

Fig. 2. (a) Ultrasonic cell crusher; (b) Amplitude lever.

power ratio/sludge volume) was adjusted to 6, 9, 12, and 15 W/L, respectively. Upon completion of the ultrasonic treatment, the pH value, temperature, specific resistance, moisture content, particle size distribution of the sludge, and moisture content of the sludge after centrifugal dewatering were measured. Subsequently, the data were analyzed and comprehensively compared in order to determine the optimal value of sound energy density for individual conditioning.

In this stage, 5 boxes of sludge were taken, with each containing 300 mL. The sound energy density was adjusted to the optimal value obtained, and the ultrasonic action time was varied at 5, 15, 30, 45, and 60 s. The aim was to determine the optimal time for ultrasonic conditioning.

2.4. *Analytical methods*

2.4.1. *Measurement of water content (WC)*

The sludge sample is placed into the centrifuge sample bottle, ensuring that four centrifuge samples are simultaneously processed with a mass difference of less than 4g between each sample. The sludge is filtered through filter cloth at the bottom. Centrifugation is carried out at 6000 r/min for 5 min, after which the moisture content of the filter cake is determined. The thermal drying method is employed to measure the moisture content of the sludge. The centrifuged sludge cake is placed in a thermostatic oven until it reaches a constant weight, and the average value is recorded.

2.4.2. *Measurement of specific resistance to filtration (SRF)*

SRF is assessed using a device specifically designed for measuring sludge specific resistance. A measuring cylinder is filled with 100 mL of sludge, which is then poured into a Buchner funnel containing filter paper. Vacuum filtration is employed under a constant pressure of 0.06 MPa. The volume of filtrate is recorded at 10-second intervals until the filter cake cracks. To mitigate the complexity and potential errors associated with the measurement of sludge specific resistance, two parallel samples are selected for the experiment, and the average value is calculated.

2.4.3. *Measurement of pH value and temperature*

Portable ion meters equipped with temperature and pH electrodes are used to measure the pH value and temperature of the sludge.

2.4.4. *Particle size analysis*

The particle size distribution of the sludge is determined using a laser particle size analyzer. The sludge sample is diluted with deionized water to achieve a concentration of 15 mg/L. Three determinations are conducted, and the average value is taken for each sample.

2.4.5. *Scanning electron microscope (SEM) analysis*

After drying the sludge sample in an oven, the sludge is analyzed using a scanning electron microscope. Various magnifications, including 200 times, 500 times, 1000 times, 2000 times, and 5000 times, are employed for the analysis.

3. Results and discussion

3.1. *Effect of ultrasonic energy density on sludge dewatering performance*

3.1.1. *Effect of water content and SRF with ultrasonic energy density*

The impact of different ultrasonic energy densities (6 W/L, 9 W/L, 12 W/L, and 15 W/L) with ultrasonic action times of 15 s and 30 s on sludge dewatering performance was investigated. Fig. 3 displays the water content of the filter cake after ultrasonic conditioning and centrifugation of the sludge. Fig. 4 presents the results of the SRF tests. These figures provide insights into the effects of ultrasonic energy density on the water content and specific resistance of the sludge during

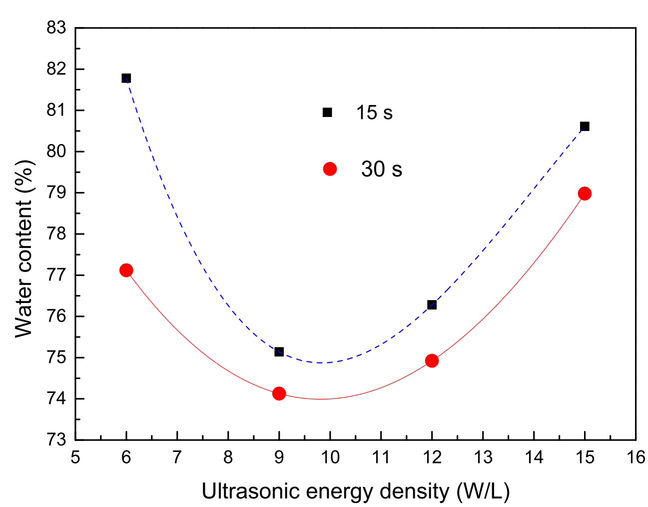

Fig. 3. Variation curve of WC with ultrasonic energy density after centrifugation.

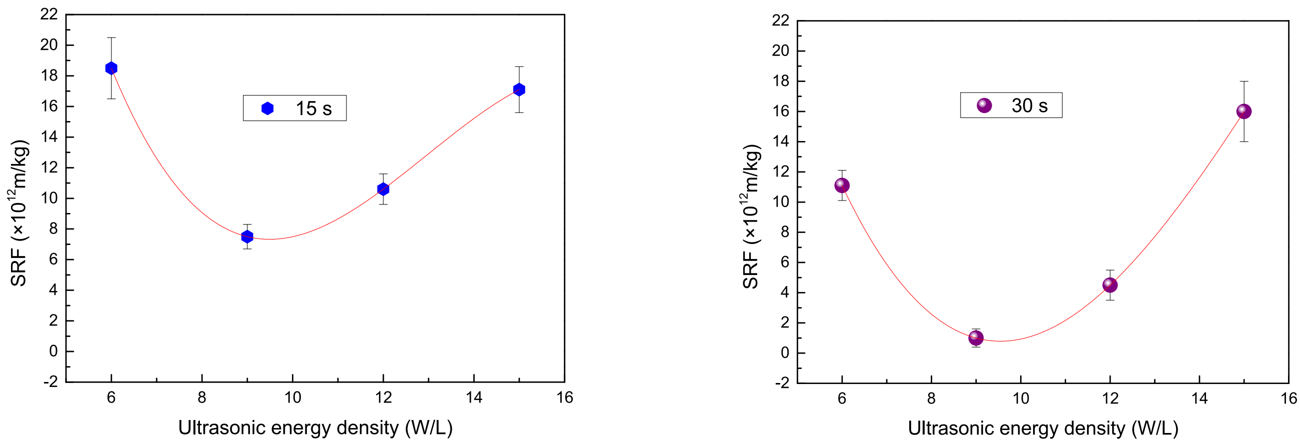

(a) (b)

Fig. 4. Variation curve of SRF with ultrasonic energy density for (a) 15 s; (b) 30 s.

the dewatering process.

Figs. 3 and 4 reveal a distinct pattern in the behavior of both WC and SRF concerning the increment in ultrasonic energy density. Initially, these parameters experience a decline followed by an increase. The optimal ultrasonic energy density for achieving minimal moisture content and SRF in the centrifuged sludge cake, after exposure to ultrasonic treatment for 15 s and 30 s, is estimated to be approximately 9.8 W. Comparing the moisture content of the centrifuged sludge cake treated with ultrasonic waves for 15 s and 30 s (measuring 74.8 % and 74.0 %, respectively) to that of the untreated cake (83.7 %), a reduction of 10.6 % and 11.6 % is observed. Within the range of ultrasonic energy density between 6 and 9.8 W/L, WC and SRF exhibit a gradual decrease, indicating an improvement in sludge dewatering performance. This suggests that as the ultrasonic energy density and treatment time increase, the diameter of sludge flocs diminishes, leading to gradual breakdown in floc structure. This breakdown is caused by the disintegration of flocs and cell structures by the ultrasonic waves. Consequently, water is released from the cells, promoting coagulation of smaller sludge particles and enhancing the overall dewatering performance of the sludge. However, WC and SRF demonstrate a gradual increase as energy density continues to rise. This increment is indicative of a decline in the sludge's dewatering performance. The underlying cause for this deterioration is the further disruption of sludge cells as both ultrasonic time and energy density increase. This disruption releases a considerable amount of protein (PN) and polysaccharides (PS), resulting in increased sludge viscosity, SRF, and MC, all contributing to the degradation of dewatering performance. [29].

Based on the observed trends, it is evident that there exists an optimal ultrasonic energy density that enhances the dewatering performance of sludge. Deviating from this optimum, either by utilizing excessively low or high ultrasonic energy densities, proves to be ineffective. In the present experiment, the optimal ultrasonic energy density for the tested sludge samples is determined to be 9.8 W. At this energy density, both the moisture content and specific resistance factor reach their minimal values, indicating the most favorable dewatering outcomes.

3.1.2. *Effect of pH value and sludge temperature with ultrasonic energy density*

Fig. 5 illustrates the variations in pH of the sludge following ultrasonic treatment.

Based on the observations from Fig. 5, it is apparent that the pH of the sludge experiences a reduction with increasing ultrasonic energy density following the ultrasonic treatment. This decrease in pH can be attributed to the disruption of sludge flocs and cell structures, resulting in the release of water and organic substances contained within the cells. These organic substances, potentially including organic acids or carbonates, contribute to the alteration of the sludge's chemical characteristics, precipitating a decline in pH. However, the magnitude of this pH reduction is not considerable. This can be attributed to the complex composition of the sludge, as well as the presence of ampholytic proteins and polysaccharides generated during the sludge disruption process, which exhibit a buffering effect, as depicted in Fig. 6 [30].

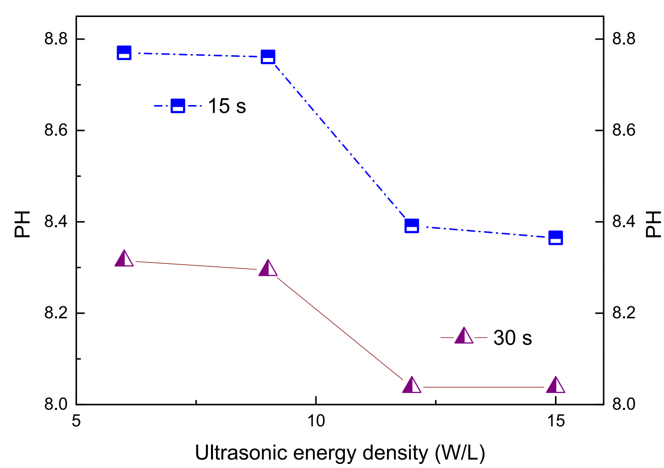

Fig. 5. Variation curve of pH value with ultrasonic energy density.

Fig. 7 depicts the temperature variation of the sludge slurry following ultrasonic treatment. As depicted in Fig. 7, the temperature of the slurry demonstrates a positive correlation with increasing ultrasonic energy density following ultrasonic treatment. The application of ultrasonic waves at a frequency of 20 kHz induces the formation of cavitation bubbles within the liquid phase. These bubbles undergo growth until reaching a critical size, followed by a forceful collapse that generates instantaneous high temperature (5000 K), high pressure, and substantial water shear forces within the surrounding liquid. Concurrently, both the particles and the medium vibrate, with the medium absorbing the vibrational energy and converting it into thermal energy, subsequently elevating the temperature of the slurry. Nonetheless, the duration of ultrasonic treatment restricts the extent of temperature

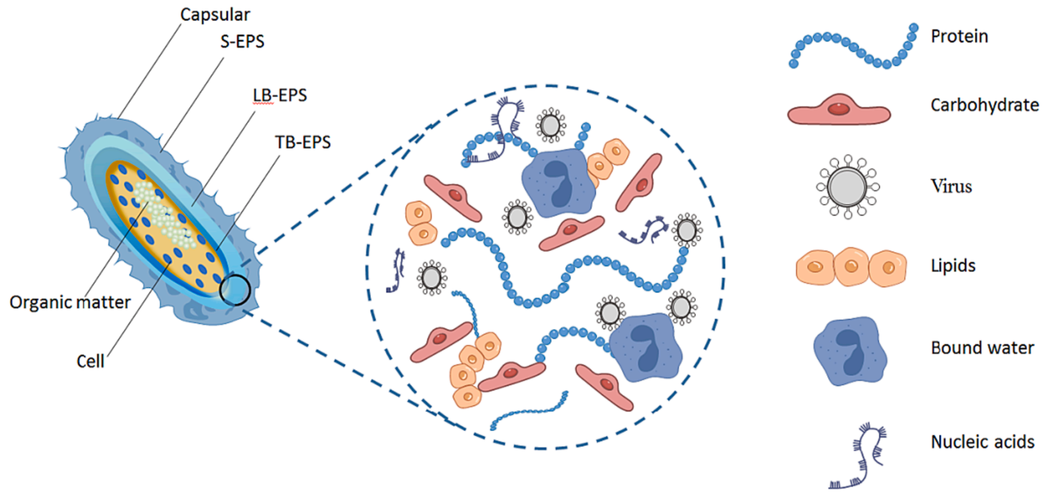

Fig. 6. Structure and composition of EPS (Lin et al., 2022).

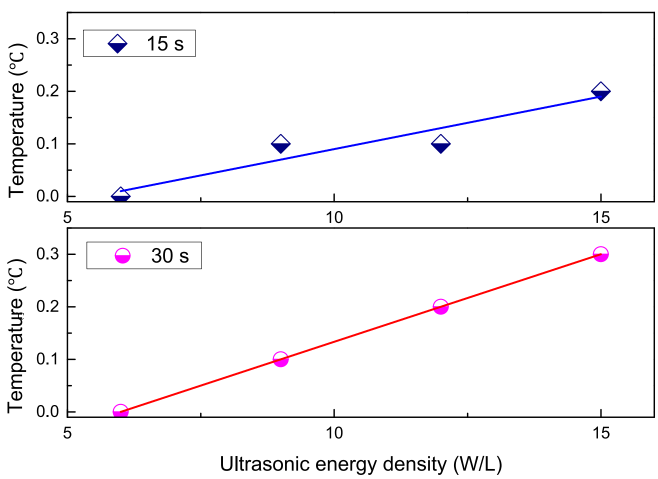

Fig. 7. Variation curve of sludge temperature with ultrasonic energy density.

increase.

3.1.3. *The effect of ultrasonic energy density on sludge particles*

The influence of ultrasonic energy density on the particle size distribution of sludge is illustrated in Fig. 8. Fig. 8a demonstrates the particle size distribution of sludge for varied ultrasonic energy densities after a 15-second ultrasonic treatment. Additionally, Fig. 8b showcases the particle size distribution of sludge under different ultrasonic energy densities following a 30-second ultrasonic treatment.

From the analysis of Fig. 8, it is evident that the particle size of the sludge predominantly lies within the range of 10——300 μm. Following ultrasonic treatment for 15 s and 30 s, at ultrasonic energy densities of 6 W, 9 W, 12 W, and 15 W, the weighted average particle size of the sludge decreases gradually from the initial size of 73.109 μm to 70.805 μm, 67.245 μm, 63.501 μm, 63.232 μm, and 70.138 μm, 65.78 μm, 61.629 μm, 59.456 μm , respectively. However, it is worth noting that the reduction in particle size becomes less pronounced as the ultrasonic energy density increases.

This phenomenon can be attributed to the compact structure and strong particle bonding within the sludge flocs prior to ultrasonic treatment. As the ultrasonic energy density intensifies, the sludge flocs progressively loosen and experience greater structural damage. Consequently, the flocs disintegrate, releasing bound water and organic

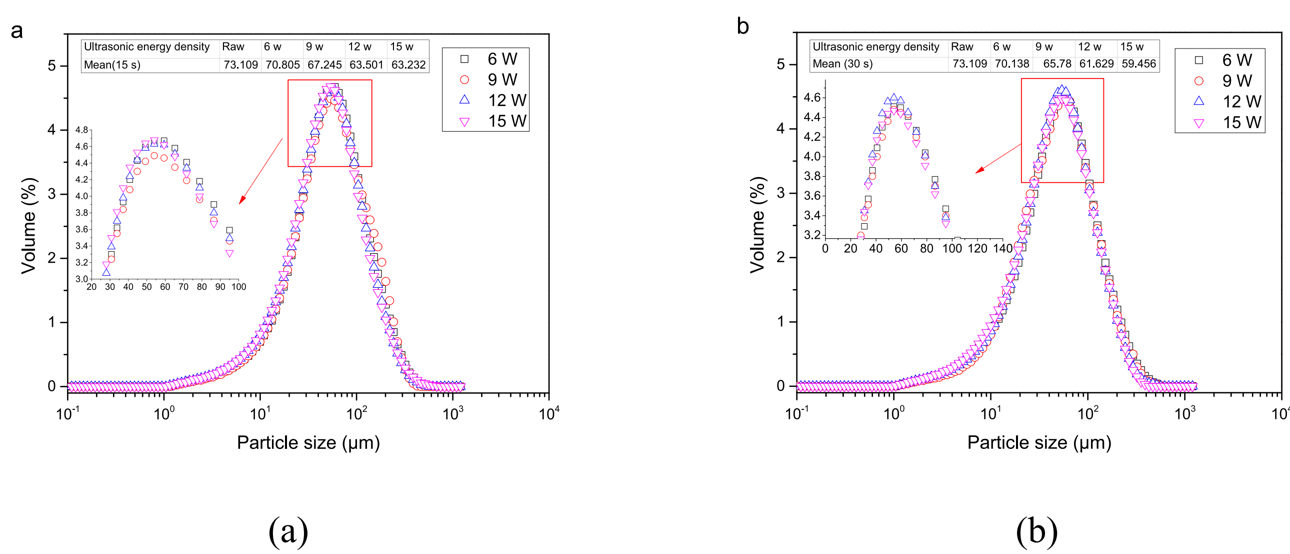

Fig. 8. Sludge particle size distribution with ultrasonic energy density for (a) 15 s ; (b) 30 s.

matter. As a result, both the floc size and sludge particle size decrease. Excessively high levels of ultrasonic energy density can cause severe damage to the floc structure, leading to further decomposition of both the flocs and organic matter. This decomposition generates minute particle fragments comprising nucleic acids, polysaccharides, proteins, lipid particles, and inorganic particles. The impact of this process is discernible in the particle size distribution, wherein the average particle size of the sludge gradually diminishes. As more sludge flocs are disrupted, the extent of particle size reduction becomes less pronounced.

3.1.4. Analysis of microscopic structure in sludge cake

The SEM images of the raw sludge, as shown in Fig. 9, illustrates that the structure of the sludge flocs remains relatively intact. The flocs consist of numerous densely packed spherical particles that are tightly adhered together, resulting in a compact structure. The sludge flocs exhibit a closely interconnected network with a relatively smooth and complete surface, effectively enveloping the microbial cells. This enclosure provides limited exposure of the microbial cells, ensuring their protection within the sludge. The interlocking sludge flocs are held together by the EPS, which form a gel matrix. This gel matrix not only encases the microbial cells but also encapsulates the inorganic particles, contributing to the stability of the floc structure. Consequently, it acts as a natural protective barrier for the microorganisms present in the sludge.

Figs. 10 and 11 showcase SEM images of sludge subjected to ultrasound treatment at power densities of 6 W/L, 9 W/L, 12 W/L, and 15 W/L for 15 s and 30 s, respectively. Fig. 10a and 11a depict the microstructure of sludge treated with a power density of 6 W/L. The images reveal a substantial exposure of intact cells, accompanied by a decreased compactness of sludge flocs and the presence of large floc aggregates. Moving on to Fig. 10b and 11b, the microstructure shows sludge treated with a power density of 9 W/L. In this case, the sludge flocs exhibit further looseness, a reduction in the particle size of sludge particles, visible disruption of the floc structure, increased exposure of EPS filamentous bacteria, ruptured cell walls, and noticeable sludge porosity.

Transitioning to Fig. 10c and 11c, these images capture the microstructure of sludge treated with a power density of 12 W/L. Here, cell walls exhibit distinct indentations and fractures, sludge flocs reassemble and combine, and sporadic instances of sludge porosity can be observed. Finally, Fig. 10d and 11d present the microstructure of sludge treated with a power density of 15 W/L. In these cases, cell walls suffer severe breakage, EPS and microbial cells on the outer layer experience rupture and inactivation, inorganic particles within the sludge aggregate and bind together with fragments of microbial cells, and small flake-like floc aggregates become visible. As a result, the sludge regains denseness, and the surface channels of the pores close.

3.2. The impact of ultrasonic duration on the sludge dewatering performance

3.2.1. Effect of water content and SRF with ultrasonic duration

Fig. 12 depicts the impact of ultrasound treatment duration on the dewaterability of sludge, measured at the optimal ultrasound power density of 9.8 W/L. Moreover, Fig. 13 showcases the variations in SRF of the sludge as a function of ultrasound treatment time, also at the optimal power density of 9.8 W/L.

Analysis of Figs. 12 and 13 reveals a consistent trend wherein the WC and SRF of the sludge gradually decline with prolonged treatment time, indicating an enhancement in dewaterability. Notably, the WC and SRF reach their minimum values after a treatment time of 30 s. However, beyond this threshold, both WC and SRF begin to increase again, suggesting a decline in dewaterability. This phenomenon signifies that extending the ultrasound treatment time beyond the optimum value adversely affects the treatment efficacy.

The excessive breakdown of sludge flocs, alteration of internal cellular structures, and release of nucleic acids, polysaccharides, proteins, fat particles, and inorganic particles due to prolonged ultrasound treatment contribute to increased sludge viscosity and modification of its chemical properties. Consequently, water re-adsorption occurs, resulting in heightened water content and diminished dewaterability. These trends underscore the existence of an optimal ultrasound treatment time, where excessively short or extended treatment times prove detrimental to improving sludge dewaterability. For the sludge samples in this investigation, the optimal ultrasound treatment time is determined to be 30 s.

3.2.2. Effect of pH and temperature with ultrasonic duration

Fig. 14 depicts the fluctuation of the pH value of the sludge as a function of ultrasound treatment time. On the other hand, Fig. 15 presents the changes in sludge temperature throughout the ultrasound treatment duration.

From the observation of Fig. 15, it is apparent that the pH value of the sludge undergoes a slight decrease as the ultrasound treatment time increases. This decrease, although not significant, suggests that the disruption of sludge flocs and cell structures caused by the ultrasound treatment can contribute to a lower pH value. This is consistent with the impact of ultrasound power density on the pH value, which also results in a slight decrease. It appears that the relationship between ultrasound treatment time and pH values follows a similar pattern to ultrasound power density.

Regarding Fig. 15, it is evident that as the ultrasound treatment time increases, the sludge temperature also rises. This temperature increase continues with higher ultrasound energy input. The propagation of ultrasound waves in the sludge causes the absorption and conversion of vibrational energy into thermal energy, leading to the elevation of the

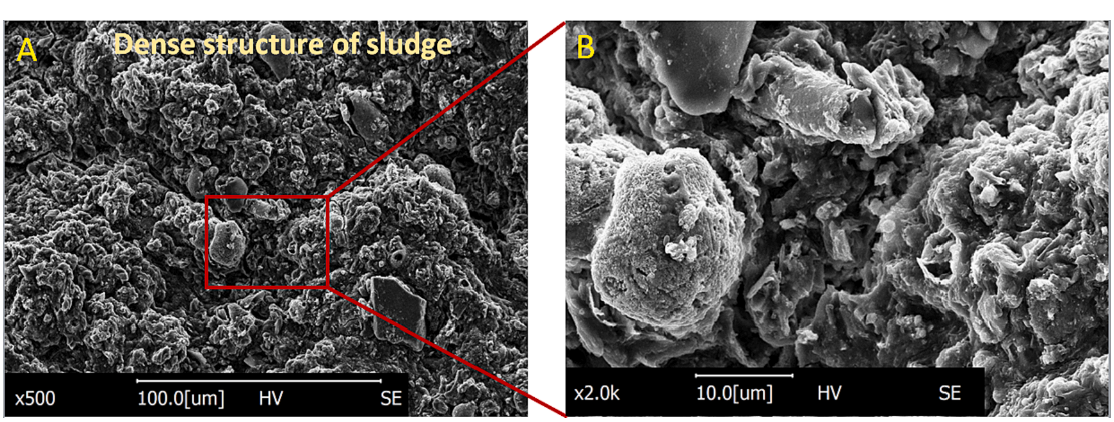

Fig. 9. SEM images of raw sludge.

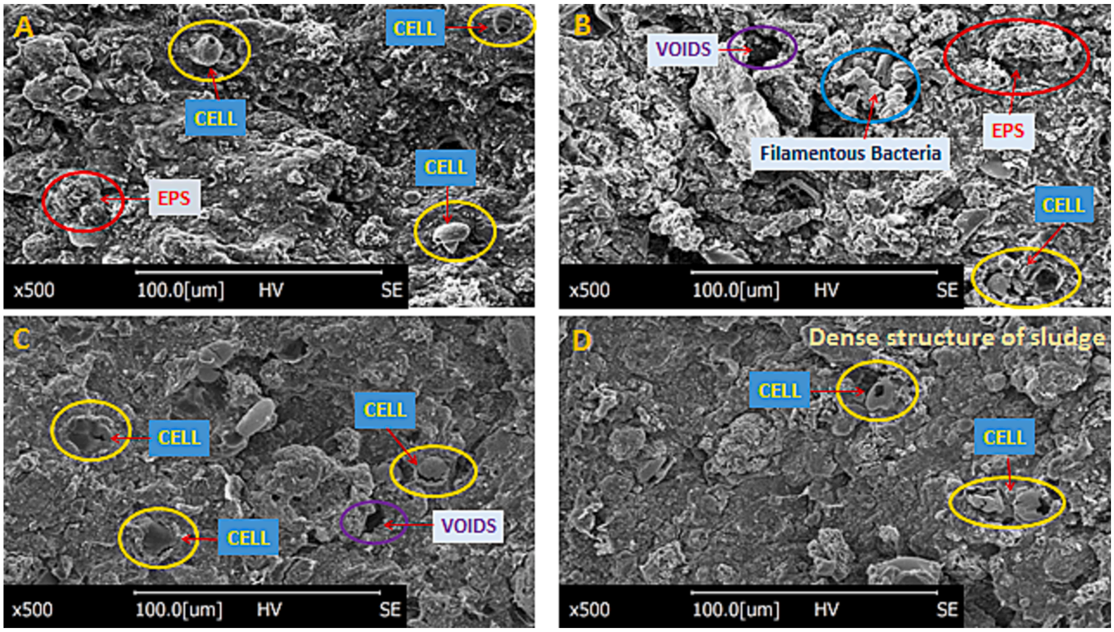

Fig. 10. SEM images of the sludge samples for 15 s US. (a) 6 W/L; (b) 9 W/L; (c) 12 W/L; (d) 15 W/L.

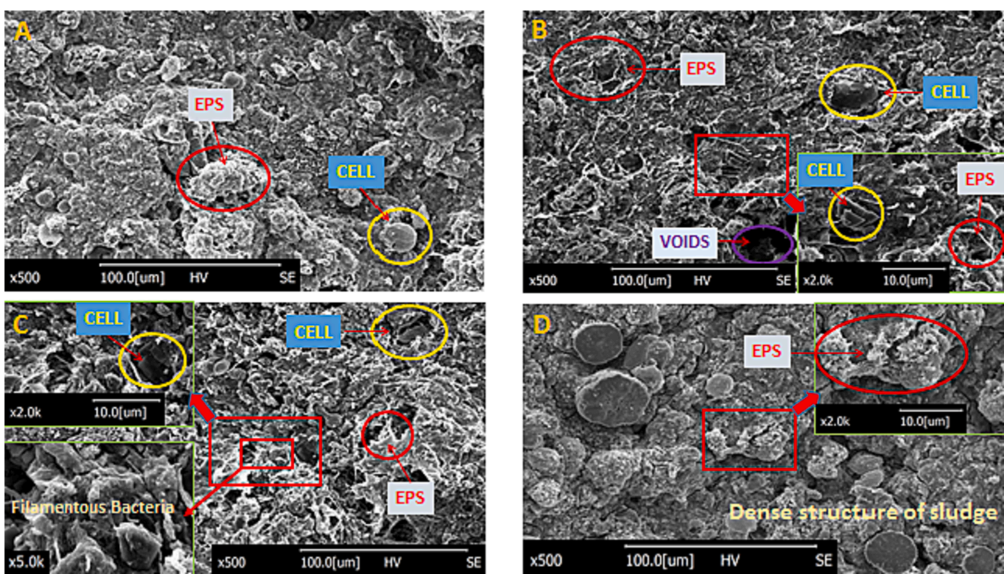

Fig. 11. SEM images of the sludge samples for 30 s US. (a) 6 W/L; (b) 9 W/L; (c) 12 W/L; (d) 15 W/L.

sludge temperature. This signifies the transformation of electrical energy into mechanical energy and, subsequently, into heat energy.

3.2.3. The effect of ultrasonic duration on sludge particles

Fig. 16 illustrates the impact of ultrasound treatment duration on the particle size distribution of sludge, considering the ideal ultrasound power density of 9.8 W/L.

Based on the findings depicted in Fig. 16, it is evident that the particle size distribution of the sludge primarily concentrates within the range of 10–200 μm. The optimal ultrasound power density of 9.8 W/L demonstrates a noteworthy influence on the sludge's weighted average particle size, as it decreases proportionately with an increase in ultrasound treatment time. Specifically, durations of 5 s, 15 s, 30 s, 45 s, and 60 s were investigated.

This phenomenon can be attributed to the fact that short-term ultrasonic treatment only affects the less cohesive flocs, leaving the stable cellular structure of the sludge relatively intact. As ultrasound treatment time prolongs, the energy input intensifies, rendering more cellular structures incapable of withstanding the instantaneous high-pressure generated by the collapse of cavitation bubbles. As a result, flocs rupture and particle size diminishes. Prolonged ultrasound treatment further amplifies energy input, leading to the complete disintegration of sludge flocs and cellular structures. Consequently, the internal structure of sludge flocs undergoes alteration, causing excessive fragmentation and consequent reduction in the average particle size.

4. Conclusion

The sludge's poor dewatering ability stems from the presence of a stable colloidal system and the tight encapsulation of bound water by EPS. EPS, which carries a negative charge, forms a stable and negatively charged colloidal system within sludge flocs. Through the mechanisms

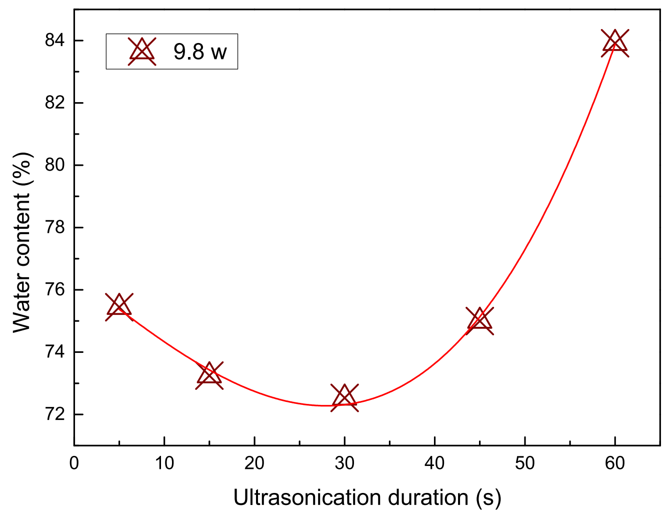

Fig. 12. Variation curve of WC with ultrasonic duration.

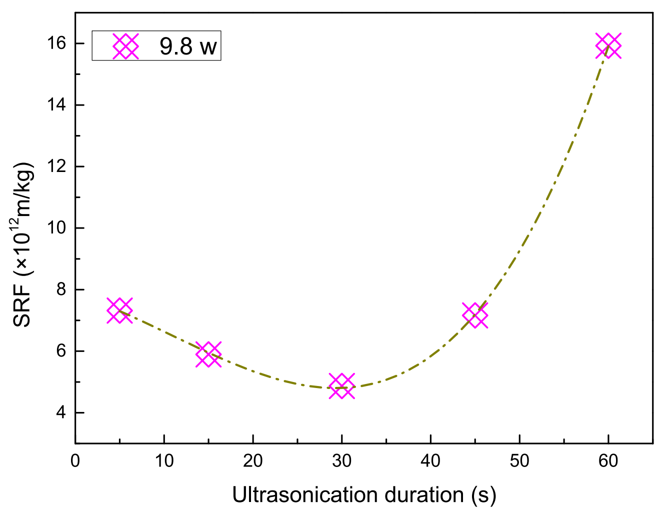

Fig. 13. Variation curve of SRF with ultrasonic duration.

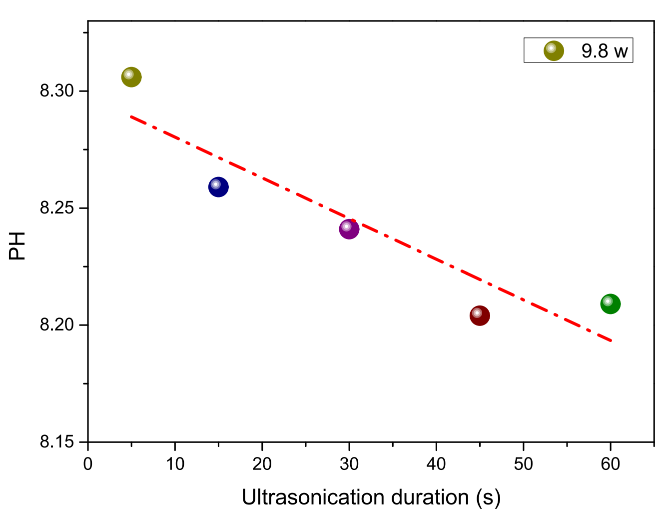

Fig. 14. Variation curve of sludge pH value with ultrasonic duration.

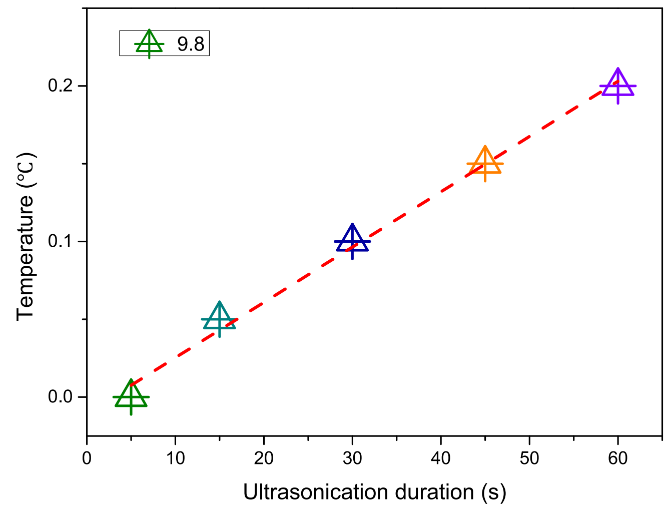

Fig. 15. Variation curve of sludge temperature with ultrasonic duration.

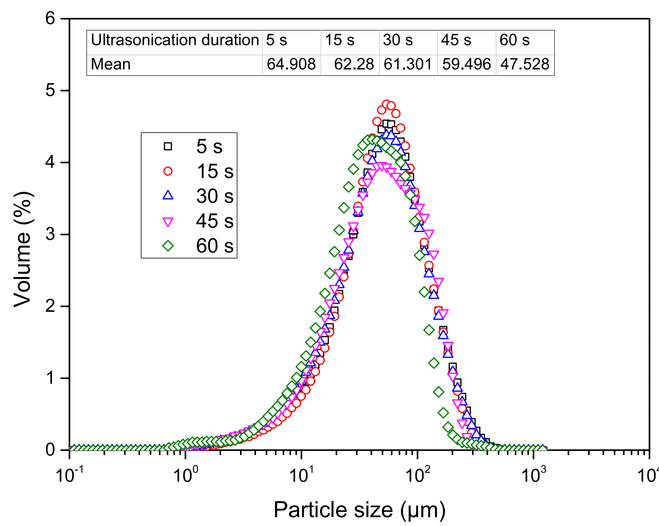

Fig. 16. Sludge particle size distribution with ultrasonic duration.

of cavitation and hydrodynamic shear, ultrasonic treatment effectively breaks down EPS, resulting in the release of tightly bound water and consequently improving the sludge's dewaterability [31].

Ultrasonic treatment exerts strong hydrodynamic shear forces, leading to the rupture of microbial cells and cell membranes present in sludge flocs. This process releases not only bound water but also organic acids or carbonates, thereby causing a decrease in the sludge's pH value. Additionally, during ultrasound treatment, the liquid phase experiences transient high temperatures and pressures, leading to a moderate temperature increase within the sludge suspension.

The effectiveness of ultrasound treatment depends on both treatment time and power density, with low-frequency ultrasound and shorter treatment times proving favorable for sludge dewatering. However, excessively high ultrasound power density or prolonged treatment time may have adverse effects on sludge dewatering performance. Therefore, it is essential to carefully select appropriate ultrasound power density and treatment time to enhance sludge dewaterability.

Furthermore, apart from improving sludge dewatering, ultrasound treatment disrupts microbial cells, releasing enzymes and other substances that hasten hydrolysis processes. This facilitates the extraction of valuable compounds from within the cells, enabling resource recovery and recycling. Consequently, ultrasound technology is expected to continue playing a crucial and unique role in sludge treatment [32,33].

CRediT authorship contribution statement

Yongzheng Qi: Conceptualization, Formal analysis, Methodology, Writing – review & editing, Writing – original draft. **Jianhao Chen:** Conceptualization, Investigation, Resources. **Haoqing Xu:** Conceptualization, Writing – review & editing. **Silin Wu:** Conceptualization, Resources, Writing – review & editing. **Ziming Yang:** Resources, Writing – original draft. **Aizhao Zhou:** Supervision, Validation. **Yunjie Hao:** Investigation, Methodology.

Declaration of competing interest

The authors declare that they have no known competing financial interests or personal relationships that could have appeared to influence the work reported in this paper.

Acknowledgments

The authors acknowledge the financial support from The Belt and Road Special Foundation of The National Key Laboratory of Water Disaster Prevention (2021491611) and the National Natural Science Foundation of China (52108369).

References

[1] M. Mobaraki, R.S. Semken, A. Mikkola, J.J.U. Pyrhönen, Enhanced Sludge Dewatering Based on the Application of High-Power Ultrasonic Vibration 84 (2018) 438–445.
[2] Y. Qi, Z. Wang, P. Jiang, Y. Guan, L. Wang, L. Mei, A. Zhou, H. Hou, H. Xu, Q. Tang, Test and Analysis of Sludge Dewatering with a Vacuum Negative Pressure Load at the Bottom of Full Section, Advances in Civil Engineering 2020 (2020) 1–12.
[3] H. Pawlak-Kruczek, K. Krochmalny, M. Wnukowski, L. Niedzwiecki, Slow Pyrolysis of the Sewage Sludge With Additives: Calcium Oxide and Lignite, J. Energy Res. Technol. 140 (2018).
[4] J. Zhang, Y. Qi, X. Zhang, G. Zhang, H. Yang, F. Nattabi, Experimental investigation of sludge dewatering for single- and double-drainage conditions with a vacuum negative pressure load at the bottom, PLoS One 16 (2021) e0253806.
[5] Y. Qi, Z. Wang, P. Jiang, Y. Guan, L. Wang, L. Mei, A. Zhou, H. Hou, H. Xu, Test and Analysis of Sludge Dewatering with a Vacuum Negative Pressure Load at the Bottom of Full Section, Advances in Civil Engineering 2020 (2020) 1–12.
[6] R. Barati Rashvanlou, H. Pasalari, A.A. Moserzadeh, M. Farzadkia, A combined ultrasonic and chemical conditioning process for upgrading the sludge dewaterability, Int. J. Environ. Anal. Chem. 102 (2020) 1613–1626.
[7] U. Menon, N. Suresh, G. George, A.M. Ealias, M.P. Saravanakumar, A study on combined effect of Fenton and Free Nitrous Acid treatment on sludge dewaterability with ultrasonic assistance: Preliminary investigation on improved calorific value, Chem. Eng. J. 382 (2020).
[8] A. Mostafa, M.-G. Kim, S. Im, M.-K. Lee, S. Kang, D.-H. Kim, Series of Combined Pretreatment Can Affect the Solubilization of Waste-Activated Sludge, Energies 13 (2020).
[9] L. Wolny, P. Wolski, Ultrasounds Energy as an Agent of Polyelectrolyte Modification Prior to Sewage Sludge Conditioning, Energies 14 (2021).
[10] H. Liu, X. Wang, S. Qin, W. Lai, X. Yang, S. Xu, E. Lichtfouse, Comprehensive role of thermal combined ultrasonic pre-treatment in sewage sludge disposal, Sci Total Environ 789 (2021), 147862.
[11] H. Pawlak-Kruczek, M. Wnukowski, L. Niedzwiecki, M. Kowal, K. Krochmalny, Gasification of Torrefied Sewage Sludge With the Addition of Calcium Carbonate, J. Energy Res. Technol. 142 (2020).
[12] H. Mao, Y. Chi, F. Wang, F. Mao, F. Liang, S. Lu, K. Cen, Effect of Ultrasonic Pre-treatment on Dewaterability and Moisture Distribution in Sewage Sludge, Waste Biomass Valoriz. 9 (2017) 247–253.
[13] T. Lippert, J. Bandelin, F. Schlederer, J.E. Drewes, K. Koch, Impact of ultrasound-induced cavitation on the fluid dynamics of water and sewage sludge in ultrasonic flatbed reactors, Ultrason Sonochem 55 (2019) 217–222.
[14] X. Xu, D. Cao, Z. Wang, J. Liu, J. Gao, M. Sanchuan, Z. Wang, Study on ultrasonic treatment for municipal sludge, Ultrason Sonochem 57 (2019) 29–37.
[15] N. Lambert, P. Van Aken, I. Smets, L. Appels, R. Dewil, Performance assessment of ultrasonic sludge disintegration in activated sludge wastewater treatment plants under nutrient-deficient conditions, Chem. Eng. J. 431 (2022).
[16] S. Wu, M. Zheng, Q. Dong, Y. Liu, C. Wang, Evaluating the excess sludge reduction in activated sludge system with ultrasonic treatment, Water Sci Technol 77 (2018) 2341–2347.
[17] X. Mou, Z. Chen, Experimental study on the effect of sludge thickness on the characteristics of ultrasound-assisted hot air convective drying municipal sewage sludge, Drying Technol. 39 (2020) 752–764.
[18] B. Bień, J.D. Bień, Analysis of Reject Water Formed in the Mechanical Dewatering Process of Digested Sludge Conditioned by Physical and Chemical Methods, Energies 15 (2022).
[19] P. Wolski, The effect of ultrasonic disintegration on sewage sludge conditioning, Desalin. Water Treat. 199 (2020) 99–106.
[20] F. Golbabaei Kootenaei, N. Mehrdadi, G. Nabi Bidhendi, H. Amini Rad, H. Hasanlou, A. Mahmoudnia, Improvement of Sludge Dewatering by Ultrasonic Pretreatment, International, J. Environ. Res. 16 (2022).
[21] J. Gao, Y. Liu, Y. Yan, J. Wan, F. Liu, Promotion of sludge process reduction using low-intensity ultrasonic treatment, J. Clean. Prod. 325 (2021).
[22] M.J. Shim, T.Y. Jung, D.H. Yoon, Y.M. Yang, J. Rumky, Y.Y. Yoon, HNO(2) treatment of sludge: An alternative way of sludge usage as fertilizer, J Environ Manage 258 (2020), 110016.
[23] M. Ruiz-Hernando, G. Martinez-Elorza, J. Labanda, J. Llorens, Dewaterability of sewage sludge by ultrasonic, thermal and chemical treatments, Chem. Eng. J. 230 (2013) 102–110.
[24] J. Gao, Y. Wang, Y. Yan, Z. Li, Ultrasonic-alkali method for synergistic breakdown of excess sludge for protein extraction, J. Clean. Prod. 295 (2021).
[25] X. Zhang, P. Ye, Y.J.J.o.E.M. Wu, Enhanced technology for sewage sludge advanced dewatering from an engineering practice perspective: A review, 321 (2022) 115938.
[26] Y. Yan, Y. Zhang, J. Wan, J. Gao, F.J.S.o.T.T.E. Liu, Optimization of protein recovery from sewage sludge via controlled and energy-saving ultrasonic-alkali hydrolysis, (2023) 162004.
[27] B.-C. You, C.-C. Huang, S.-H.-J.-B.-T. Chuang, The Characteristics of Stepwise Ultrasonic Hydrolysates of Sludge for Enhancing Denitrification 370 (2023), 128566.
[28] V.H.P. To, T.V. Nguyen, S. Vigneswaran, H.H. Ngo, A review on sludge dewatering indices, Water Sci. Technol. 74 (2016) 1–16.
[29] Y. Yang, X. Yang, Q. Yang, H. Zhang, W. Xu, L. Zhu, P. Ma, Y. Li, Exploring the feasibility and potential mechanism of synergistic enhancement of sludge dewaterability by ultrasonic cracking, chitosan re-flocculation and sludge-based biochar adsorption of water-holding substances, J. Environ. Chem. Eng. 10 (2022), 108303.
[30] W. Lin, X. Liu, A. Ding, H.H. Ngo, R. Zhang, J. Nan, J. Ma, G. Li, Advanced oxidation processes (AOPs)-based sludge conditioning for enhanced sludge dewatering and micropollutants removal: A critical review, J. Water Process Eng. 45 (2022), 102468.
[31] J. Zhang, Y. Dong, S. Wang, X. Liu, L. Lv, G. Zhang, Z. Ren, Comparison of ultrasonic treatment of primary and secondary sludges: Physical properties and chemical properties, Sep. Purif. Technol. 308 (2023), 122892.
[32] C.B. Alvim, M. Bes-Piá, J.A. Mendoza-Roca, An innovative approach to the application of ultrasounds to remove polyethylene microspheres from activated sludge, Sep. Purif. Technol. 264 (2021), 118429.
[33] R. Zhang, Y. Mao, L. Meng, Excess sludge cell lysis by ultrasound combined with ozone, Sep. Purif. Technol. 276 (2021), 119359.